ICCSE'21 International Conference on Contemporary approach on revolutionary Science and Engineering, April 9-10, 2021 ISBN: 978-81-910765-1-6

Spin-Lattice Relaxation Measurements and Structural Elucidation of VO(II) ion Doped in a Paramagnetic Host by EPR Study

K. Senthil Kumaran[1], S. Boobalan[2]*, G. Sivasankari[3]

[1,2]*Research and Development Centre, Bharathiyar University, Coimbatore – 641046, India.*

[1]*Department of Chemistry, SNS College of Eng. Coimbatore – 641107, India.*

[3]*Department of Chemistry,Cauvery College for women, Trichy – 620018, India.*

[1]sivakspm@gmail.com

[3]gsivasankari.chem@cauverycollege.ac.in

[*2]*Department of Chemistry, Indra Ganesan College of Engineering, Trichy-620012, India.*

[2]sivaboobalan@gmail.com

Abstract— **Electron Paramagnetic Resonance (EPR) studies provide a great deal of information about the magnetic properties of paramagnetic ion in different host lattices. They also lead to understanding of the nature of the bonding of the metal ion with its ligands [1]. The EPR spectroscopic investigation of VO(II) ion doped in a paramagnetic host lattice, Triaquapotassiumbismalonatonickelate complex has been carried out at room temperature using X-band spectrometer to gain information about location of the impurity and bond characters. Single crystal rotated along the three orthogonal crystallographic axes has yielded spin Hamiltonian parameters g and A as: g_{xx} = 1.979, g_{yy} = 1.968, g_{zz} = 1.936 and A_{xx} = 6.92, A_{yy} = 6.02, A_{zz} = 18.12 mT respectively. Single crystal EPR spectra further indicate the presence of vanadyl impurity in a single site. Angular variation studies in all the three orthogonal planes confirm that the VO(II) ion has occupied an interstitial position in the lattice. The spin Hamiltonian parameters indicate orthorhombic nature of the impurity. The analysis of powder spectrum also reveals the presence of only one site. The isofrequency plots and powder spectrum have been simulated to confirm the spin-Hamiltonian parameters. The percentage of covalency of metal-oxygen bond has been estimated. The admixture coefficients have also been calculated.**

Keywords— **1. Inorganic complex 2. Vanadyl ion 3. Crystal growth 4. Electron Paramagnetic Resonance 5. location**

I. INTRODUCTION

Electron Paramagnetic Resonance (EPR) yields a great deal of information about the magnetic properties of paramagnetic ion in different host lattices. They also lead to some understanding of the nature of the bonding of the metal ion with its ligands. The EPR studies of paramagnetic ion doped in diamagnetic host yields important information about the magnetic properties of matter, chemical bonding, dynamic interactions of spins with lattice, nuclear moments, the possibility of nuclear alignment and orientational properties of the host lattice [1-3]. The observed resonances are sharp, due to the absence of dipole – dipole broadening. Alternatively, it is necessary in a few cases, to dope a paramagnetic impurity into a paramagnetic host lattice. In this situation, the dipole-dipole interaction between the two paramagnetic centres will help to estimate relaxation times. However, reasonably sharp EPR lines are seen even in paramagnetic lattice [4-8], if the paramagnetic host does not show its characteristic EPR spectra at room temperature, but provide resonances only at low temperature.

Vanadium is one of the transition group elements that have been studied with EPR spectroscopy in divalent, trivalent and tetravalent states. The tetravalent state, V^{4+} exists as VO(II) ion with a single unpaired d-electron. The $3d^1$ configuration of vanadyl ion allows electron paramagnetic resonance to be observed at ambient temperatures [9-11]. The behaviour of vanadyl complex is dictated by the strong V=O bonding and most of the complexes possess C_{4v} symmetry. EPR studies of VO(II) ion in a variety of host lattices have been reported [12-19]. However, in a recent work [20], both substitutional and interstitial sites for VO(II) impurity are reported. Therefore, interest is developed to ensure the location of the impurity ion and nature of bonding in TPMN single crystal. In this chapter we report the EPR and optical absorption studies of VO(II) ion in TPMN single crystal and deduce the spin Hamiltonian, spin-lattice relaxation time measurement and molecular orbital (MO) coefficients. These MO coefficients are further used to discuss the nature of bonding of VO(II) ion with different ligands in the crystal. Triaquapotassiumbismalonatonickelate is abbreviated here as TPMN.

II. MATERIALS AND METHODS

A. Preparation of single crystal of VO(II)-doped $[K(H_2O)_{3/2}]_2[Ni(mal)_2]$:

Malonic acid, nickel(II) basic carbonate, potassium hydrogen carbonate were purchased from commercial sources and used as received. $[K(H_2O)_{3/2}]_2[Ni(mal)_2]$ was synthesized by adding solid nickel(II) basic carbonate to an aqueous solution of malonic acid under continuous stirring. The suspension was heated at 40 – 50 °C, until a colourless solution was obtained. This solution was filtered and mixed with an aqueous solution of potassium hydrogen carbonate. The solution was then filtered and doped with five different concentrations of vanadyl sulfate

 ISBN: 978-81-910765-1-6

(0.05, 0.1, 0.15, 0.2 and 5.0%). All the crystals were transparent and blue colour with well shaped and separated out on concentrating the solution at room temperature.

B. EPR Measurements:

The EPR spectra are recorded at 300 K on a JEOL JES-TE100 ESR spectrometer operating at X-band frequencies, having a 100 kHz field modulation to obtain the first-derivative EPR spectrum. 1,1-Diphenyl-2-picrylhydrazyl (DPPH) with a g-value of 2.0036 is used as a reference for g-factor calculations.

C. UV-Visible, FT-IR, Powder XRD Measurements:

The optical spectrum has been recorded at room temperature using a Varian Cary 5000 ultraviolet-visible (UV-Vis) near-infrared spectrophotometer in the range of 200-1300 nm. In the present investigation, the FT-IR spectra are recorded for doped and undoped materials on a Shimadzu FT-IR-8300/8700 spectrometer, in the frequency range of 4000-400 cm^{-1}. The measurements are made using almost transparent KBr pellets containing fine-powdered samples at room temperature. In the current study, powder XRD studies are carried out for doped and undoped materials on a PANalytical X'pert PRO diffractometer with Cu Kα radiation of wavelength λ = 0.15406 nm, 2θ values between 5-75°, at room temperature.

III. Crystal Structure

TPMN, $[K(H_2O)_{3/2}]_2[Ni(mal)_2]$ is isostructural with $[K(H_2O)_{3/2}]_2[Cu(mal)_2]$ [21]. It belongs to orthorhombic crystal system with space group Pbcn, having unit cell parameters a = 0.7398 nm, b = 1.8830 nm, c = 0.9320 nm, $\alpha = \beta = \gamma = 90°$, and Z = 4. Each copper atom is six coordinated and exhibit a 4+2 elongated octahedron environment. Four carboxylate-oxygen atoms from two bidentate malonate ligands define the equatorial plane around the copper atom. Apical positions are occupied by two symmetry related carboxylated-oxygen atoms from other two monodentate malonate ligands.

IV. Results and Discussions

A. EPR Studies:

The EPR studies on the single crystal doped with diluted paramagnetic impurity yielded interesting results. As the crystals were grown with five different concentrations, crystals with 0.05 and 0.1% concentration show weak lines; whereas crystals with 0.2 and 5.0% gave relatively broad lines. Hence, in all the further EPR measurements, crystals with concentration of 0.15% are used. However, 0.2% concentration samples are used for powder XRD measurements and 5.0% samples are employed for optical measurements. A good, well-shaped single crystal of optimum size have been chosen and rotation are done in three orthogonal axes namely a, b and c. Generally one could expect eight lines for a vanadyl ion due to the interaction of electronic spin (S = ½) with the nuclear spin (I = 7/2). During the crystal rotations in the three orthogonal planes namely ab, bc and ac, a maximum of eight lines are only noticed in each plane, indicates the presence of only one type of the impurity in the crystal.

Fig. 1 Single crystal EPR spectrum of VO(II)/TPMN when the applied magnetic field is 50º away from the crystallographic axis a in ab plane. Frequency = 9.05989 GHz.

A typical EPR spectrum of VO(II) doped in TPMN, when the applied external magnetic field (B) is parallel to crystallographic axis a is given in Fig. 1. It consists of sharp eight resonance lines. Fig. 2 is showing the EPR spectrum recorded in ac plane, when the applied magnetic field (B) is 140º away from the axis c, corresponding to maximum hyperfine separation. The bc plane

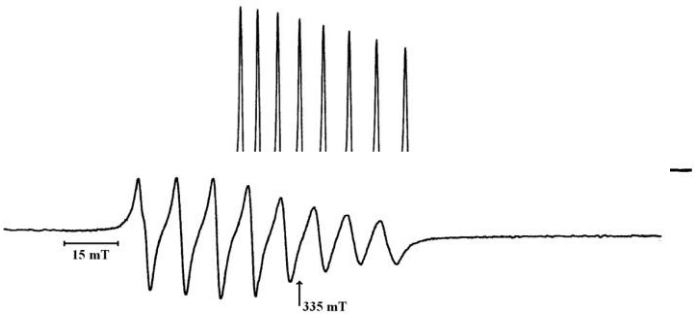

is almost identical with ac plane. Fig. 3 is showing an EPR spectrum of bc plane, when the applied magnetic field (B) is 50º away from the axis c, corresponding to broad resonances, due to the presence of dipolar-dipolar interaction between the host–guest paramagnetic centres. In single crystal of TPMN doped with VO(II), reasonably sharp EPR lines are observed in all the three crystallographic planes except in few orientations, having dipolar broadening due to the paramagnetic host–impurity interaction. However, the line width of the hyperfine lines of TPMN is found to be larger than those found in the corresponding diamagnetic lattice. This is due to the presence of the Ni(II) ion interaction with the vanadyl ion. Crystal rotations are done in all the three planes and to obtain isofrequency plots, for all the three planes, calculate the spin Hamiltonian parameters (g and A matrices).

Fig. 2 Single crystal EPR spectrum of VO(II)/TPMN recorded at room temperature when the magnetic field is perpendicular to crystallographic axis c in ac plane. Frequency = 9.06020 GHz.

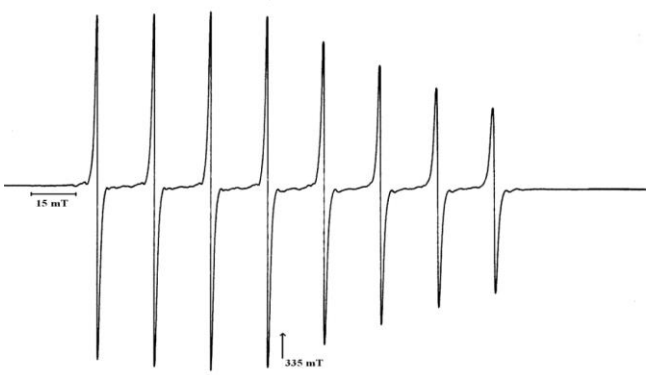

Fig. 3 Single crystal EPR spectrum of VO(II)/TPMN recorded at room temperature when the applied magnetic field is parallel to crystallographic axis c. Frequency = 9.05926 GHz.

1) *Calculation of spin-Hamiltonian parameters:* In order to obtain spin Hamiltonian parameters, the spectra obtained on the orthogonal planes for VO(II) ion was fitted with the following spin Hamiltonian.

$$\hat{H} = \beta(g_x B_x S_x + g_y B_y S_y + g_z B_z S_z) + A_x S_x I_x + A_y S_y I_y + A_z S_z I_z \quad (1)$$

The spin Hamiltonian parameters (g and A matrices), calculated using the program EPR-NMR [22], with orthorhombic g and A matrices, are given in Table 1 along with the direction cosines. The direction cosines of the principal g and A are nearly

 ISBN: 978-81-910765-1-6

coincident. Since the maxima and minima of g and A variation are obtained at the same angle. For comparison, the direction cosines of Ni –O bonds in TPMN are given in Table 2. These are helpful to predict the location of the paramagnetic impurity. If the direction cosines of g match with one of the direction cosines of Ni – O bonds, a substitution location can be suggested. Otherwise, the impurity might have entered an interstitial location. A close look at the direction cosines given in Table 1 and 2, indicate that none of them matches well with each other. In other words, one can suggest that the vanadyl ion might have entered the lattice in an interstitial location. The spin Hamiltonian values agree well with the literature values, a few of which are summarized in Table 3. Using the g and A matrices, the angular variation plots are simulated and it is found to fit with the experimental values. In general, if a paramagnetic system exhibits axial symmetry, the isofrequency plots in ac and bc planes will be identical, whereas the resonance lines in ab plane show invariance. Most of the systems studied so far for VO(II) fall under this category. On the other hand, a slight deviation from axial symmetry makes the resonance lines in ab plane show angular dependence. In the present system, the isofrquency plot in ab plane is angle dependent and isofrequency plots in ac and bc planes are not identical. This immediately confirms that the impurity has rhombic symmetry. In the Figs. 4 – 6, the solid lines indicate the theoretical values and the solid circles indicate the experimental values. A good agreement is obtained.

2) *Polycrystalline studies:* To confirm the single crystal analysis, powder EPR spectrum, recorded at room temperature, is given in Fig. 4.7. It clearly indicates eight parallel and eight perpendicular features, typical of vanadyl impurity in axially symmetric form. The spin Hamiltonian parameters calculated from the powder spectrum are also given in Table 4.3. The agreement between the powder data and single crystal data is excellent. However, g_{xx}/g_{yy} and A_{xx}/A_{yy} are not resolved in powder spectrum due to the closeness in their values. This type of observation is very common in VO(II) ion impurity. The powder spectrum is simulated using the program SimFonia and the agreement is good, further confirming our values.

TABLE I
THE SPIN HAMILTONIAN PARAMETERS OBTAINED FROM THE SINGLE CRYSTAL ROTATIONS FOR VO(II) DOPED IN TPMN USING PROGRAM EPR-NMR [22].

	Principal values	Direction cosines		
		a	b	c
g matrix				
1.959 0.006 0.016	1.979	-0.4249	0.5354	-0.7298
1.964 -0.014	1.968	-0.7041	-0.7022	-0.1052
1.959	1.936	-0.5689	0.4692	0.6755
A matrix (mT)				
10.87 -3.18 -4.45	6.92	0.3459	-0.5429	0.7651
9.43 3.85	6.02	-0.7198	-0.6767	-0.1547
10.77	18.12	-0.6017	0.4973	0.6249
Powder spectrum $g_{\parallel} = 1.995$ $g_{\perp} = 1.973$ $A_{\parallel} = 18.31$ mT $A_{\perp} = 6.99$ mT				

TABLE II
THE DIRECTION COSINES OF NI-O BONDS AND K-O BONDS FOR TPMN, OBTAINED FROM THE CRYSTALLOGRAPHIC DATA.

Ni-O, K-O bonds in TPMN	Direction cosines a	b	c
Ni-O (1)	0.3684	0.7375	0.6076
Ni-O (2)	0.4611	-0.7192	0.5232
Ni-O (3)	0.3881	0.5304	0.7537
K(1)-O(1)	0.2492	-0.8895	0.4111
K(1)-O(4)	0.2486	-0.8789	0.4072
K(1)-O(1w)	0.0000	1.0000	0.0000
K(1)-O(2w)	-0.1869	-0.9621	-0.1986
K(2)-O(2)	0.4345	1.1675	0.4930
K(2)-O(4)	0.4736	0.4166	0.7759
K(2)-O(2w)	-0.6303	-0.3930	-0.6695

3) Admixture coefficients: We have also calculated the admixture coefficients from the spin Hamiltonian parameters. The single unpaired electron on the metal ion occupies d_{xy} or d_{xz} or d_{yz} orbital in an octahedral configuration. Upon lowering of symmetry, the groung state d_{xy}, when acted upon by spin-orbit term can mix with $d_{x^2-y^2}$, d_{yz} and d_{xy}. If C_1, C_2 and C_3 are the admixture coefficients, where the ground state d_{xy} can mix with $d_{x^2-y^2}$, d_{yz} and d_{xy}: these are related to the spin-Hamiltonian parameters by the relations [25].

$$g_{\parallel} = 2\left(3C_1^2 - C_2^2 - 2C_3^2\right) \quad (2)$$

$$g_{\perp} = 4C_1\left(C_2 - C_3\right) \quad (3)$$

These equations along with the normalization condition $\left(C_1^2 + C_2^2 + C_3^2 = 1\right)$ can be solved iteratively to obtain the admixture coefficients. The values thus obtained are given in Table 4, along with the data obtained for other systems. Using these coefficients and spin Hamiltonian parameters, two more parameters κ (a dimension less constant describing core s-polarisation) and P have also been calculated using the equations (4) and (5)

$$A_{\parallel} = P[g_{\parallel} - (\kappa + (15/7)(1 - 2C_3^2) - (3/7)(1 + C_1C_2C_3)] \quad (4)$$

$$A_{\perp} = P[(11/14)g_{\perp} - 2C_1C_2(\kappa + (9/7)] \quad (5)$$

and these values are also given in Table 4.

TABLE III
SPIN HAMILTONIAN PARAMETERS OF VO(II) IN TPMN AND OTHER RELATED HOST LATTICES

Host lattice	g_{xx}	g_{yy}	g_{zz}	A_{xx}	A_{yy}	A_{zz}	Ref.
$H_2Co(C_4H_2O_4)_2 \cdot 6H_2O$ (site I)	1.975	2.061	1.935	7.1	7.9	18.8	[5]
(site II)	1.985	2.005	1.932	6.7	7.7	18.8	
HCS[a] (site I)	1.995	1.985	1.941	7.5	7.7	18.9	[23]
(site II)	1.986	1.979	1.941	7.3	7.7	18.6	
Cosacpy[b] (site I)	2.001	1.989	1.938	7.3	5.2	18.7	[24]
(site II)	2.001	1.987	1.923	7.2	7.4	19.9	
TPMN	1.979	1.968	1.936	6.9	6.0	18.1	Present work

[a] Hexaimidazol cobalt sulphate
[b] Tetraaquabis (pyridine) Co(II) saccharinate tetrahydrate

 ISBN: 978-81-910765-1-6

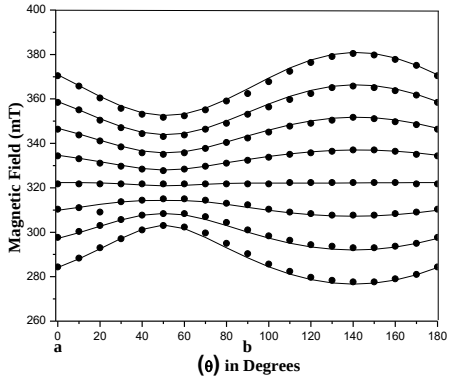

Fig. 4 Angular variation of hyperfine lines for c axis rotation of the VO(II)/TPMN single crystal at room temperature. The solid circles and lines correspond to experimental and theoretical values respectively. Frequency = 9.05989 GHz.

4) Evaluation of MO coefficients:

The spin-Hamiltonian parameters are related to the molecular orbital coefficients by the following expression [28]

$$g_{\parallel} = g_e - 8\beta_1^2 \beta_2^2 \lambda/(\Delta E_1(b_2 - b_1^*) \quad (6)$$

$$g_{\perp} = g_e - (2\lambda\beta_2^2 e_{\pi}^2/\Delta E_2(b_2 - e_{\pi}^*) \quad (7)$$

$$A_{\parallel} = -p\kappa - (4/7)\beta_2^2 p - (g_e - g_{\parallel})P - (3/7)(g_e - g_{\parallel})P \quad (8)$$

$$A_{\perp} = -p\kappa + (2/7)\beta_2^2 p - (11/14)(g_e - g_{\perp})P \quad (9)$$

Where β_1^2 , β_2^2 and e_{π}^2 are molecular orbital coefficients. The isotropic EPR parameters, using the relations

$$g_0 = (1/3)(g_{\parallel} + 2g_{\perp}) \quad (10)$$

$$A_0 = (1/3)(A_{\parallel} + 2A_{\perp}) \quad (11)$$

Combining the above relations with the expressions (4.8) and (4.9) we get $A_0 = -P\kappa - (g_e - g_0)P$ (12)

Using the above equation, the value of Fermi contact term is calculated. The Fermi contact term is directly related to the isotropic hyperfine coupling and represents the amount of unpaired electron density at the nucleus [29]. Combining Eq. (8) and (9) and eliminating κ one can get an expression for β_2^2 in term of the g and A tensor values.

$$\beta_2^2 = (-7/6)[(A_{\parallel} - A_{\perp})/P + (g_e - g_{\parallel}) - (5/14)(g_e - g_{\perp})] \quad (13)$$

Using the above relation β_2^2 is calculated. The deviation of β_2^2 from unity usually represents the degree of admixture of the ligand orbital and increase in the degree of covalency. The present value of β_2^2 = 0.93 clearly indicates that the bonding is nearly ionic and represents poor π bonding of the ligands. The β_2^2 should be equal to unity for a nonbonding orbital in the case of pure $VO(H_2O)_5^{2-}$ complex [30].

Fig. 5 Angular variation of hyperfine lines for b axis rotation of the VO(II)/TPMN single crystal at room temperature. Frequency = 9.06020 GHz.

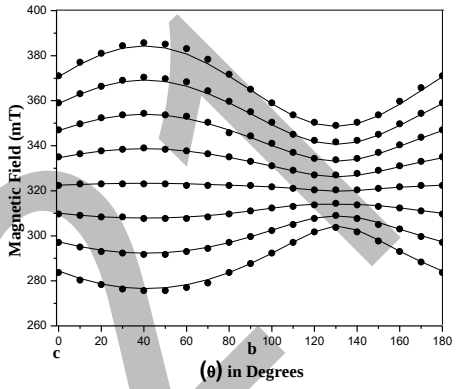

Fig. 6 Angular variation of hyperfine lines for a axis rotation of the VO(II)/TPMN single crystal at room temperature. Frequency = 9.05926 GHz.

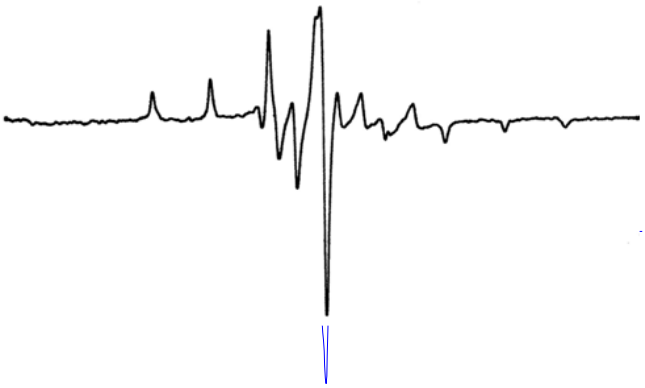

Fig.7 Powder EPR spectrum of VO(II)/TPMN at room temperature. Top figure corresponds to experimental one, whereas bottom one is the simulated using powder values. Frequency = 9.35653 GHz.

TABLE IV
ORBITAL ADMIXTURE COEFFICIENTS AND BONDING PARAMETERS FOR A FEW VANADYL IONS.

Host lattice	C_1	C_2	C_3	κ	$P\times10^{-4}$ cm^{-1}	Ref.

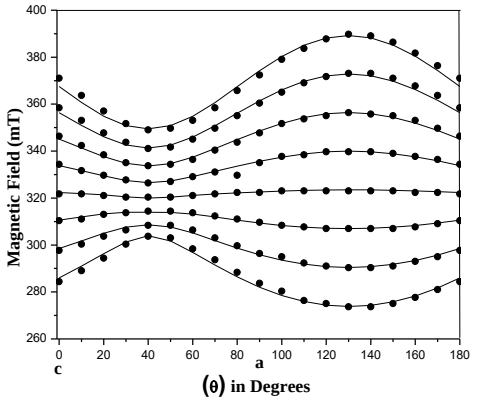

 ISBN: 978-81-910765-1-6

$MgK_2SO_4.6H_2O$	0.700	0.713	0.040	0.85	133.1	[20]
HCS	0.702	0.711	0.042	0.87	130.0	[23]
MAPH[c]	0.702	0.711	0.040	0.91	112.0	[26]
CAPH[d]	0.702	0.711	0.040	0.88	125.7	[27]
TPMN	0.702	0.712	0.040	0.84	110.0	Present work

TABLE 5
MOLECULAR ORBITAL COEFFICIENTS OF VO(II) DOPED IN TPMN.

Host lattice	β_1^2	β_2^2	e_π^2	Ref.
$KZnClSO_4.3H_2O$	0.91	1	0.68	[15]
POM	0.86	1	0.86	[19]
LAM Site I Site II	0.26 0.68	1	0.62 0.95	[31]
Sodium citrate Site I Site II	0.91 0.88	1	0.68 0.71	[32]
TPMN	0.94	0.93	0.89	Present Work

β_1^2 indicate the delocalisation in the σ system. The in-plane σ bonding varies from compound to compound and decreases from unity as the covalency of the bond increases. From Eq. (6), the value of β_1^2 is calculated and found to be 0.94. β_1^2 values reported in different hosts are collected in Table 5 and are compared with the present value. Considerable contribution of 4s spin density to κ is predicted from the value of β_1^2. The out-of-plane π bonding represented by e_π^2 is calculated from Eq. (7). The calculated value of 0.89 is comparable with many other systems.

5) Spin – lattice relaxation time:

To study the nature and extent of dipolar interaction of the paramagnetic ion is interesting when it is incorporated in a paramagnetic host. At room temperature, the Ni(II) is EPR silent, and this helps us to successfully analyze the data at this temperature. The tremendous change in the line width is noticed as the temperature is reduced. A few spectra are given in Fig. 8. Hence, this dramatic change in line width during cooling of the sample can be ascribed to the influence of the paramagnetic host. In other words, this is due to the dipolar-dipolar interaction between the paramagnetic impurity VO(II) and the paramagnetic host Ni(II). As the temperature is reduced, the nickel ion becomes EPR active at low temperature and overlaps with the resonance lines due to vanadyl ion, thus causing broadness. The line-width variation of VO(II) hyperfine lines in paramagnetic lattice can be understood on the basis of host spin-lattice relaxation mechanism. The fast spin-lattice relaxation of the host ions can randomly modulate the dipolar interaction between the paramagnetic host and the impurity ions resulting in "Host spin-lattice relaxation narrowing" [33]. When the spin-lattice relaxation narrowing mechanism is effective, the host spin-lattice relaxation time (T_1) is given by [33]

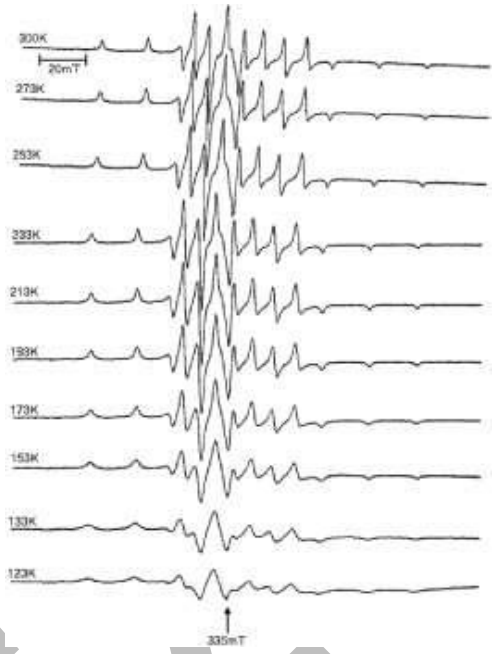

Fig. 8 Variable temperature powder EPR spectra of the VO(II)/TPMN. These spectra have been used to calculate relaxation times. υ = 9.11963 GHz.

$$T_1 = \frac{3}{7}\frac{h}{2g_h\beta}\frac{\Delta B_{imp}}{Bd_d^2} \qquad (14)$$

$$Bd_d^2 = 5.1(g_h\beta n)^2 S_h (S_h + 1)$$

Where, g_h = the host g value
S_h = the effective host spin and it is taken to be ½
n = the number of host spins per unit volume which can be calculated from the crystallographic data of the crystal lattice (0.8423×10^{24}) and
ΔB_{imp} = the impurity line width.

The calculated spin-lattice relaxation times T_1 are plotted as a function of temperature and the graph indicates that as the temperature decreases the spin-lattice relaxation time T_1 increases, as shown in Fig. 9. The order of spin-lattice relaxation time obtained in our work is found to be agreeable with the values reported for Ni(II) host in literature [33]. The T_1 value varies

from 0.12×10^{-12}s at 300 K to 0.21×10^{-12}s at 148 K. These relaxation times are so short and may be due to the overlap of resonance lines of the host and the impurity, which corresponds to cross-relaxation mechanism.

2. *Optical studies:*

The optical absorption spectrum of vanadyl doped TPMN single crystal is recorded at room temperature is given in the Fig. 10. The spectrum consists of three characteristic bands at 272, 382 and 689 nm, respectively. The first two peaks correspond to d –d transitions in vanadyl. The band at 689 nm corresponds to the transition $b_2 - e_\pi^*$ and the band at 382 nm is due to the transition $b_2 - b_1^*$ levels. The higher energy band at 272 nm can be assigned to a charge transfer (CT) band due to the promotion of the electron from the filled bonding level (oxygen orbital) to the nonbonding orbital (d_{xy}) level [34].

 ISBN: 978-81-910765-1-6

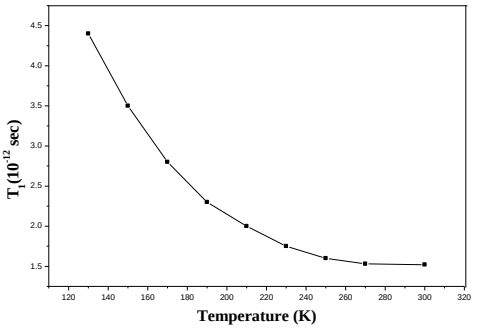

Fig. 9 Plot of host spin-lattice relaxation time (T_1), derived using line-width of the VO(II)/TPMN, as a function of temperature.

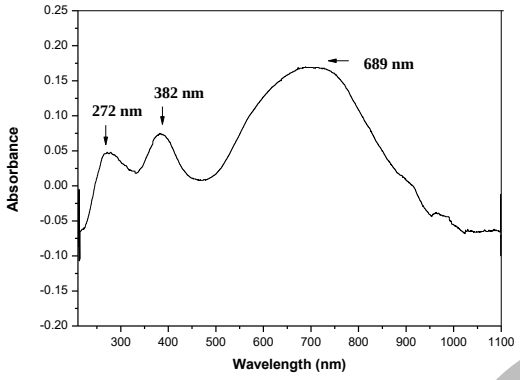

Fig. 10 Optical absorption spectrum of VO(II)/TPMN recorded at room temperature.

Tables must be numbered using uppercase Roman numerals. Table captions must be centred and in 8 pt Regular font with Small Caps. Every word in a table caption must be capitalized except for short minor words as listed in Section III-B. Captions with table numbers must be placed before their associated tables, as shown in Table 1.

*1) **Spin – orbit coupling:***

EPR data and optical absorption data are combined together to calculate the spin orbit coupling constant (λ). For an electron in the d_{xy} ground state, neglecting the covalence effects the g tensor values related to the optical transitions are given by

$$g_{\parallel} = g_e - (8\lambda/\Delta E_1(b_2 - b_1^*) \quad (15)$$

$$g_{\perp} = g_e - (2\lambda/\Delta E_2(b_2 - e_{\pi}^*) \quad (16)$$

where g_e is the free electron g value of 2.0023. Here, one can take $g_{\parallel} = g_{zz}$ and $g_{\perp} = (g_{xx} + g_{yy})/2$. Using the above equations (15) and (16) $\lambda = 115$ cm^{-1} is obtained. The value of $\lambda = 170$ cm^{-1} is reported for VO(II) [35, 36]. Such a drastic reduction in the value of λ observed in the present study indicates the substantial π bonding in the vanadyl complex.

3. FT-IR studies:

The infrared absorption spectrum is the most useful technique to identify the functional groups and to know the molecular structure. The FT-IR spectra of pure and VO(II) doped TPMN at room temperature is shown in Fig. 11. It shows the bands in the range 3600 – 2400, 2500 – 2000, 1750 – 1250, 1100 – 400 cm^{-1}. Observed FTIR bands and their tentative assignments for pure TPMN and VO(II) doped TPMN are tabulated in Table 6. Carboxylic acid shows broad and intense O – H stretching absorption in the region of 3400 – 2500 cm^{-1}. The bands observed at 3350, 3250 cm^{-1} are due to the O – H bonding corresponding to water ligation [37]. The bands at 1690 and 1590 cm^{-1} are assigned to C =O and C = C stretching, respectively. The twin bands at 1400 and 1440 cm^{-1} are due to O – H bending vibration. The C –H bending vibrations are generally observed in the 1370 – 1220 cm^{-1} wavenumber region. The bands at 1370 and 1270 cm^{-1} have been assigned to C –H bending vibrations. The bands at 1180, 1110 and 987 cm^{-1} have been assigned to O – H out-of-plane deformation bands. The bands observed at 779, 737 and 698 are attributed as out-of-plane C –H bending vibration. The bands at lower wavenumber region from 600 to 400 cm^{-1} are due to O –H deformation bands.

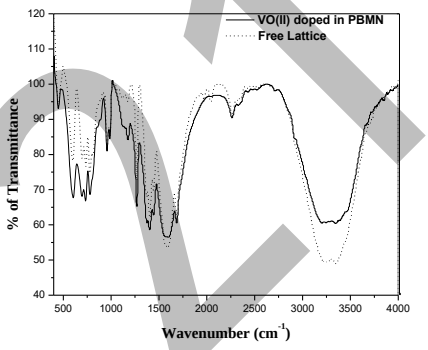

Fig. 11 FT-IR spectrum of VO(II)/TPMN recorded at room temperature.

TABLE 6
OBSERVED FTIR BANDS AND THEIR TENTATIVE ASSIGNMENTS FOR PURE TPMN AND VO(II) DOPED TPMN. (BR-BROAD, SH-SHARP, W-WEAK)

Band Positions (cm^{-1})		Assignments
Pure TPMN	VO(II) doped TPMN	
3350 (br)	3350 (br)	O –H stretching
3250 (br)	3250 (br)	
2270 (w)	2270 (w)	C – H stretching
2040 (w)	2040 (w)	
1970 (w)	1970 (w)	
1690 (sh)	1690 (sh)	C =O stretching
1590 (sh)	1590 (sh)	C - C stretching
1440 (sh)	1440 (sh)	O – H bending
1400 (sh)	1400 (sh)	
1370 (sh)	1370 (sh)	C – H bending
1180 (sh)	1180 (sh)	O – H out of plane deformation
1110 (sh)	1110 (sh)	
987 (sh)	987 (sh)	
779 (sh)	779 (sh)	C –H out of plane bend

B. Powder XRD studies:

Powder XRD pattern of VO(II) doped TPMN at room temperature is shown in Fig. 12. According to powder XRD measurements [38], VO(II) doped TPMN powder sample has identical lattice parameters as TPMN powder sample, as expected from the low impurity concentration. The lattice parameters are tabulated in Table 8 with the single crystal XRD parameter of TPMC [21]. It is clear from the table 6 that the parameters of TPMN and VO(II) doped TPMN matched with reported values of copper complex [21], confirming that the zinc

 ISBN: 978-81-910765-1-6

complex is isomorphic with copper complex and the low dopant concentration of VO(II) in TPMN does not alter the symmetry of host lattice.

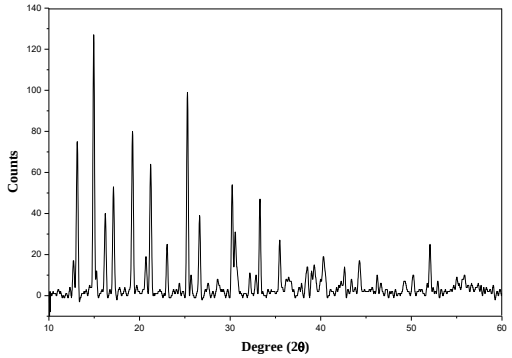

Fig. 12 Powder XRD pattern of VO(II)/TPMN recorded at room temperature.

TABLE 7
THE CALCULATED LATTICE PARAMETERS OF TPMN AND VO(II) DOPED TPMN FROM POWDER XRD, ALONG WITH SINGLE CRYSTAL XRD OF TPMC [21].

Lattice parameters (nm) of TPMC from single crystal XRD	Lattice parameters (nm) calculated from	
	TPMN	VO(II) doped TPMN
a = 0.7398	a = 0.7482	a = 0.7482
b = 1.8830	b = 1.8924	b = 1.8924
c = 0.9320	c = 0.9823	c = 0.9823

V. CONCLUSION

Single crystal vanadyl ion doped TPMN has been studied at room temperature using EPR technique indicates that only one site in the lattice and the number of sites seems to be independent of concentration of the impurity. The spin Hamiltonian parameters indicate that the impurity is rhombically distorted and entered the lattice in an interstitial position. The angular variation plot and the powder EPR spectrum have been simulated, which authenticates evaluated spin Hamiltonian parameters. The optical absorption spectrum at room temperature shows three bands characteristic of vanadyl ions in distorted octahedral symmetry. By using EPR and optical data, admixture coefficients, molecular orbital coefficients, Fermi contact term and dipolar interaction parameter have also been calculated. FTIR and XRD studies confirm the formation and structure of the complex.

ACKNOWLEDGMENT

We acknowledge Pondicherry University to record experimental data.

REFERENCES

[1] R.S. Alger, Electron Paramagnet Resonance: Techniques and Application, Wiley, New York, 1968.
[2] J.A. Weil, J.R. Bolton, Electron Paramagnetic Resonance, Wiley, New York, 1994.
[3] V. Somasekharm, P. Sivaprasad, K. Ramesh, Y.P. Reddy, Phys. Scr., 33 (1986) 169.
[4] K.V. Narashimhulu, J. Lakshmana Rao, Spectrochim. Acta, A53 (1997) 2605.
[5] N.O. Gopal, K.V. Narasimhulu, J. Lakshmana Rao, Physica B, 307 (2001) 117.
[6] V.K. Jain, J. Chem. Phys., 84, (1986) 1994.
[7] P. Chand, V.K. Jain, G.C. Upreti, Magn. Reson. Rev., 14, (1988) 49.
[8] S.K. Misra, J. Sun, X. Li, Physica B, 168 (1991) 170.
[9] S. Dhanuskodi, A.P. Jeyakumari, Spectrochim. Acta, A57 (2001) 971.
[10] S. Deepa, K. Velavan, I. Sougandi, R. Venkatesan, P.S. Rao, Spectrochim. Acta, A61 (2005) 2482.
[11] B. Karabulut, A. Tufan, Spectrochim. Acta, A65 (2006) 742.
[12] A.K. Viswanath, J. Chem. Phys., 67 (1977) 3744.
[13] B.P. Maurya, A. Punnoose, M. Umar, R.J. Singh, Solid State Commun., 89 (1994) 59.
[14] P.A.A. Mary, S. Dhanuskodi, Spectrochim. Acta, A57 (2001) 2345.
[15] B.D.P. Raju, K.V. Narasimhulu, N.O. Gopal, J.L Rao, J. Phys. Chem. Solids, 64 (2003) 1339.
[16] R. Kripal, P. Singh, J. Mag. Magn. Mater., 307 (2006) 308.
[17] C. Shiyamala, S. Mithira, B. Natarajan, R.V.S.S.N. Ravikumar, P.S. Rao, Phys. Scr., 74 (2006) 549.
[18] B. Natarajan, S. Mithira, S. Deepa, R.V.S.S.N. Ravikumar, P.S. Rao, Radiat. Eff. Defects Solids, 161 (2006) 177.
[19] R. Kripal, M. Maurya, H. Govind, Physica B, 392 (2007) 281.
[20] H. Anandalakshmi, R. Venkatesan, T.M. Rajendiran, P.S. Rao, Spectrochim. Acta, A56 (2000) 2617.
[21] F.S. Delgado, C. Ruiz, J. Sanchiz, F. Lloret, M. Julve, Cryst. Eng. Comm., 8, (2006) 507.
[22] F. Clark, R.S. Dickson, O. B. Fulton, J. Isoya, A. Lent, D. G. Mc Gavin, M. J. Mombourquette, R. H. D. Nuttall, P. S. Rao, H. Rinnerberg, W.C. Tennant, J. A. Weil, EPR-NMR Program, University of Saskatchewan, Saskatoon, Canada, 1996.
[23] I. Sougandi, K. Velavan, R. Venkatesan, and P. Sambasiva Rao, Phys. Stat. Sol., (b)241 (2004) 3014.
[24]E. Bozkurt, B. Karabulut, I. Kartal, Y.S. Bozkurt, Chem. Phys. Lett., 477 (2009) 65.
[25] V.P. Seth, S.K. Yadav, V.K. Jain, Pramana, J. Phys., 21 (1983) 65.
[26] I. Sougandi, R. Venkatesan, T.M. Rajendiran, P. Sambasiva Rao, Phy. Scr., 67 (2003) 153.
[27] C. Shiyamala, T.M. Rajendiran, R. Venkatesan, P. Sambasiva Rao, Cryst. Res. Technol., 37 (2002) 841.
[28] A.H. Maki, B.R. McGarvey, J. Chem. Phys., 31 (1958) 35.
[29] A. Kasiviswanath, S. Radhakrishna, J. Phys. Chem. Solids, 52 (1991) 232.
[30] S.G. Sathyanarayana, V.G. Krishnan, G.S. Sastry, J. Chem. Phys., 65 (1976) 4181.
[31] R. Kripal, I. Mishra, S.K. Gupta , M. Arora, Spectrochimica Acta, A71 (2009) 1969.
[32] R. Kripal, I. Mishra, Spectrochimica Acta, A72 (2009) 538.
[33] T. Mitsuma, J. Phy. Soc. Jpn., 17 (1962) 128; S.K. Mishra, Magn. Reson. Rev., 12 (1987) 191; V.K. Jain, J. Mag. Reson., 64 (1985) 512.
[34] A.B.P. Lever, Inorganic Electronic Spectroscopy, 2nd ed, Elsevier, New York, 1986.
[35] T.M. Dunn, Trans. Faraday Soc., 57 (1961) 1441.
[36] D. Kivelson, S.K. Lee, J. Chem. Phys., 41 (1964) 1896.
[37] K. Nakamoto, P.J. McCarthy, A. Ruby, A.E. Martell, J. Am. Chem. Soc., 83 (1961) 1066.
[38] B. D. Cullity, Elements of X-ray Diffraction, Addison Wesley, Massachusetts, USA, 1978.